AIMS Mathematics, 10(5): 10340–10358.
DOI: 10.3934/math.2025471
Received: 10 December 2024
Revised: 19 April 2025
Accepted: 29 April 2025
Published: 06 May 2025

https://www.aimspress.com/journal/Math

Research article

Viscoelastic Pasternak foundation analysis of a thermoelastic microbeam using Moore–Gibson–Thompson heat conduction under Klein–Gordon (KG) nonlocality

Ahmed Yahya[1], Adam Zakria[1,*], Ibrahim-Elkhalil Ahmed[1], Shams A. Ahmed[1], Husam E. Dargail[1], Abdelgabar Adam Hassan[1] and Eshraga Salih[2]

[1] Department of Mathematics, College of Science, Jouf University, Sakaka, 2014, Saudi Arabia
[2] Department of Mathematics, College of Science, Qassim University, Buraydah, Saudi Arabia

* **Correspondence:** Email: azsidig@ju.edu.sa.

Abstract: This study sought to examine the behavior of thermoelastic microbeams supported by a viscoelastic Pasternak foundation via the Moore–Gibson–Thompson heat conduction equation within the framework of Klein–Gordon nonlocality, a novel approach for analyzing heat transfer in elastic materials. This model facilitates a more precise comprehension of the thermoelastic vibrations in microbeams. We wanted to examine the impact of foundation characteristics and thermal relaxation durations on the vibration frequency and stability of the microbeam. The Laplace transform technique was used. A graphic representation of the computed temperature, bending displacement, and moment is shown. The results provide significant insights into the design and enhancement of microbeams in advanced engineering applications, including microelectromechanical systems and nanoscale structures, where temperature effects and foundational interactions are critical. Furthermore, the fluctuation of waves is somewhat reduced in the examined model.

Keywords: thermoelastic; Klein–Gordon nonlocality; microbeams; foundation; viscoelastic; Pasternak foundation; Moore–Gibson–Thompson
Mathematics Subject Classification: 74-10, 74B05, 74F05, 74H15

1. Introduction

In recent years, microbeams have grown to be vital because of their widespread use in technology,

communication systems, electromechanical measuring devices, and magnetometers. Resonators—which can be generally manufactured from single-crystal silicon cloth via semiconductor production techniques—are used as elements of radio frequency filters for the detection of charge, force, pressure, and acceleration at center frequencies in the order of megahertz or even gigahertz. Many interesting papers have been published in this area of research [1–3]; several researchers have researched microbeams in mechanical, aeronautical, and nuclear engineering [4–6]. The differential quadrature approach was used to examine finite Euler–Bernoulli beam transverse vibration frequencies on parameter viscoelastic foundations [7,8].

The significance of research on beams resting on two-parameter elastic foundations cannot be overstated. Previous studies [9,10] that examined the behavior and diverse characteristics of such beams are of utmost importance to design and related fields. They provide crucial insights to several engineering sectors, particularly in the dynamic behavior analysis of beams situated on thermoviscoelastic foundations. In [11], the authors explored the features of a foundational model that incorporated a standard technique for bending beams on an elastic base alongside the two-parameter viscoelastic foundation, further underscoring the significance of this research. Similarly, Pradhan and Murmu [12] highlighted the effects of adhesive foundations on the deflection patterns of mechanical systems and precise mechanics.

The thermoelasticity theory is a mixture of elasticity and heat conduction theories. A thermal constitutive equation is employed by the classical coupled theory of thermoelasticity [13] in addition to its mechanical constitutive equation for the stress tensor. Some studies have been conducted on these generalized theories, such as the L–S theory developed by Lord and Shulman [14], the G–L theory presented by Green and Lindsay [15], and the G–N theory provided by Green and Naghdi [16]. The theory of classical dynamical thermoelasticity (CTE) was examined by Biot and Willis [17]. Furthermore, Tzou [18] introduced a novel dual-phase-lag (DPL) model that allows lag durations that simulate the temperature gradient and heat flow by including a new establishing component in Fourier's equation. Green and Naghdi [19,20] generated a generalized thermoelastic model. Three theories have been defined as a consequence: the first generation (GN-I) was supplied by Green and Naghdi, who went on to establish the second generation (GN-II) and the third generation (GN-III).

The number of studies devoted to Moore–Gibson–Thompson theory has increased significantly since its creation. It has also become a fascinating topic for scientists, with multiple studies concentrating on model formulation. For example, in [21–23], the authors constructed the theory's theoretical components. Several researchers have also used this theory in practice, with various thermoelastic models and certain presumptions [24,25]. The problem of thermoelasticity was studied and numerically analyzed by Bazarra et al. [26], who used the Moore–Gibson–Thomson equation to describe the thermal law. Owing to the intricate nature of the model, the topic of microbeams situated on a two-parameter and Moore–Gibson–Thompson (MGT) model and subjected to initial thermal stress has not been widely studied. Nevertheless, our study delved deeply into this subject. Various foundation models have been examined, employing numerical and analytical approaches to conduct free vibration analyses of numerous structures. Consequently, incorporating thermal coupling into the equation offers a novel approach for addressing vibration issues in structures supported by elastic foundations.

The nonlocal theory of continuum mechanics of thermoelasticity is crucial to material research. This study provides a complete foundation for understanding material behavior under thermal and mechanical loading. Nonlocal elasticity theories were established in [27,28]. Famous researchers, such

as Zhou et al. [29] and Song et al. [30], have used elasticity to address dynamic issues. The linear theory of nonlocal elasticity was used to demonstrate elastic wave dispersiveness owing to nonlocal factors in [31]. Recently, Singh et al. [32] examined how nonlocal factors affect harmonic wave propagation in elastic materials with voids. In [33,34], the nonlocal elasticity of thermoelastic materials was enhanced. Researchers have focused on wave propagation in nonlocal thermoelasticity, e.g., Biswas [35], Lata and Singh [36], and Abd-Alla et al. [37]. Jangid et al. [38] studied flat harmonic waves via Moore–Gibson–Thompson thermoelasticity with Klein–Gordon (KG) nonlocality to explore the thermal variables of thermoelastic microbeams supported by a two-parameter viscoelastic Pasternak foundation. The present paper develops the governing equations of Moore–Gibson–Thompson thermoelasticity with nonlocality to explore possible effects inspired by [39,40] Klein–Gordon-type nonlocal elasticity.

In this work, the motivation arises from the necessity for precise and realistic modeling of microbeams for advanced technological applications, whereas the challenge lies in the complex mathematical framework needed to capture the interaction of multiple sophisticated physical phenomena at small scales. The Pasternak foundation analysis of a thermoelastic microbeam was examined using various foundation models (FMs) and the Moore-Gibson-Thompson (MGT) model incorporating KG nonlocality. This study followed a structured approach: Section 2 introduces the formulation of the problems and fundamental equations. Section 3 examines the analytical solution and initial and boundary conditions of thermoelastic coupling and its impact on the transient behavior of microbeams resting on a two-parameter viscoelastic Pasternak foundation via the Moore–Gibson–Thompson heat conduction equation under KG nonlocal. As demonstrated in Section 4, the Laplace transform technique was utilized to solve the equilibrium system. Section 5 presents an analysis and discussion of the response of the studied field variables through various subsections. Finally, Section 6 summarizes the most critical conclusions drawn from the study.

2. Governing equations

We investigate the thermoelasticity and dynamics of a thin microbeam resonator that is thermoelastic and has a rectangular cross-section of length $L(0 \le x \le L)$, width $b(-\frac{b}{2} \le y \le \frac{b}{2})$, and beam thickness $h(-\frac{h}{2} \le z \le \frac{h}{2})$ by a cross-section of area $A = hb$. We specify the x-coordinate along the beam's axis, and the consistent y- and z-coordinates represent the width and thickness behavior. With an elastic modulus E and a Poisson's ratio of v, the beam is composed of a flexible material with homogenous, linear properties. A homogeneous, three-characteristic elastic soil supports the beam. The essential model is defined by the damping coefficient τ_0, the linear modulus K_1, and the Pasternak foundation coefficient K_2.

The displacement vector's components are as follows, which were attained via the Euler–Bernoulli beam theory (see [41–43]):

$$u = -z\frac{\partial w}{\partial x}, v = 0,\ w(x, y, z, t) = w(x, t). \tag{1}$$

The fundamental equation that results from applying Eq (1) to a one-dimensional problem is as follows:

$$\left(1 - e_0\nabla^2 + \tau^2\ \frac{\partial^2}{\partial t^2}\right) t_{ij} = \sigma_x = -E\left[\frac{\partial^2 w}{\partial x^2} + \alpha_T\theta\right]. \tag{2}$$

where t_{ij} are stress tensor components for nonlocal elasticity of the Klein–Gordon type, σ_x is the nonlocal axial stress, e_0 is the characteristic internal length scale parameter due to nonlocality in space, and τ is the characteristic time scale parameter due to nonlocality in time and $\alpha_T = \alpha_t/(1-2\nu)$. From Eq (2), we obtain the flexure moment M in the form

$$M(x,t) = -IE\left[\frac{\partial^2 w}{\partial x^2} + \alpha_T M_T\right], \tag{3}$$

where

$$M_T = \frac{12}{h^3}\int_{-h/2}^{h/2}\theta(x,z,t)zdz.$$

The initial magnetic field H, the current density J, the beam thickness h, and elastic modulus E are what causes this phenomenon. For a homogeneous and electrically perfect conducting thermoelastic material, the Maxwell's equations may be applied as follows:

$$\begin{gathered} J = \nabla \times h,\ \nabla \times E = -\mu_0\frac{\partial h}{\partial t},\ E = -\mu_0\left(\frac{\partial u}{\partial t}\times H\right), \\ h = \nabla\times(u\times h),\ \nabla\cdot h = 0. \end{gathered} \tag{4}$$

According to studies by Kerr [44], the fundamental Winkler elastic model is the initial model, in which the vertical displacement is intended to be commensurate with the contact pressure at any given position. With the irrelevant contact between the beam and the ground taken into consideration, the interaction between the beam and the supporting foundation can only be squeezed and follows the Pasternak three-parameter model.

$$R_f = K_1 w(x,t) - K_2\frac{\partial^2 w(x,t)}{\partial x^2}, \tag{5}$$

where w is the lateral deflection and where R_f is the foundation response per component area. The crosswise response of microbeams' equation of motion may be expressed as

$$\frac{\partial^2 M}{\partial x^2} - R_f + f(x) = \rho A\frac{\partial^2 w}{\partial t^2}, \tag{6}$$

where the longitudinal magnetic force is included as a function of space in $f(x)$. Since f_z is a body force and $f(x)$ is the force per length, in this case, $f(x) \neq f_z$, $f(x)$ may be expressed as

$$f(x) = Af_z = A\mu_0 H_x^2\frac{\partial^2 w}{\partial x^2}. \tag{7}$$

By substituting Eqs (3), (5), and (8) into Eq (7), we obtain the nanobeam motion equation as

$$\frac{\partial^4 w}{\partial x^4} - \left(\frac{K_2}{IE} + \frac{A\mu_0 H_x^2}{IE}\right)\frac{\partial^2 w}{\partial x^2} + \frac{\rho A}{IE}\frac{\partial^2 w}{\partial t^2} + \frac{K_1}{IE}w + \alpha_T\frac{\partial^2 M_T}{\partial x^2} = 0. \tag{8}$$

The generalized form of Moore–Gibson–Thompson thermoelasticity with Klein–Gordon nonlocality and heat sources is as follows [39,45]:

$$K\left(K\frac{\partial}{\partial t} + K^*\right)\left(\frac{\partial^2 \mathrm{T}}{\partial x^2} + \frac{\partial^2\theta}{\partial z^2}\right) = \left(\frac{\partial^2}{\partial t^2} + \tau_\theta\frac{\partial^3}{\partial t^3}\right)\left[\rho C_E\frac{\partial\theta}{\partial t} + \gamma T_0\frac{\partial e}{\partial t}\right], \tag{9}$$

where K is the thermal conductivity and K^* is the conductivity rate parameter.

The specific cases are as follows: $\tau_\theta \neq 0,\ K \neq 0\ and\ K^* \neq 0$, conventional thermoelastic theory (CTE) can be applied if $\tau_\theta = 0, K^* = 0,$ Lord and Shulman (LS) theory can be applied if $K^* = 0$, Green-Naghdi (GN-II) theory can be applied if $\tau_\theta = 0,\ K = 0$, and the Green-Naghdi (GN-III) model can be applied if $\tau_\theta = 0$.

Replacing Eq (1) into (9), we obtain the generalized heat conduction equation in the following form:

$$\left(K\frac{\partial}{\partial t}+K^*\right)\left(\frac{\partial^2 \mathrm{T}}{\partial x^2}+\frac{\partial^2\theta}{\partial z^2}\right)=\left(\frac{\partial^2}{\partial t^2}+\tau_\theta\ \frac{\partial^3}{\partial t^3}\right)\left[\frac{\rho C_E}{K}\frac{\partial\theta}{\partial t}-\frac{\gamma\, T_0}{K}z\frac{\partial}{\partial t}\left(\frac{\partial^2 w}{\partial x^2}\right)\right]. \tag{10}$$

3. Analytical solution

The increasing temperature for a specific microbeam varies along the thickness direction in an irregular method [2]. That is

$$\theta(x,z,t)=\theta(x,t)\sin\left(\frac{\pi z}{h}\right). \tag{11}$$

When Eq (11) is substituted into Eq (8), the motion equation (8) may be stated as follows:

$$\frac{\partial^4 w}{\partial x^4}-\left(\frac{K_2}{IE}+\frac{A\mu_0 H_x^2}{IE}\right)\frac{\partial^2 w}{\partial x^2}+\frac{\rho A}{IE}\frac{\partial^2 w}{\partial t^2}+\frac{K_1}{IE}w+\frac{24\alpha_T}{h\pi^2}\frac{\partial^2\theta}{\partial x^2}=0. \tag{12}$$

Moreover, the flexure moment M provided by Eqs (3) and (11) is

$$M(x,t)=-IE\frac{\partial^2 w(x,t)}{\partial x^2}-\frac{24IE\alpha_T}{h\pi^2}\theta. \tag{13}$$

The result attained by integrating Eq (12) with respect to z across the beam thickness from $-h/2$ to $h/2$ is

$$\left(K\frac{\partial}{\partial t}+K^*\right)\left(\frac{\partial^2}{\partial x^2}-\frac{\pi^2}{h^2}\right)\theta=\left(\frac{\partial^2}{\partial t^2}+\tau_\theta\frac{\partial^3}{\partial t^3}\right)\left[\frac{1}{k}\frac{\partial\theta}{\partial t}-\frac{\gamma\, T_0\pi^2 h}{K}\frac{\partial}{\partial t}\left(\frac{\partial^2 w}{\partial x^2}\right)\right]. \tag{14}$$

We use the following dimensionless variables below:

$$\begin{gathered}\{x',z',u',w'\}=\frac{1}{\mathrm{L}}\{x,z,u,w\},\ \theta'=\frac{\theta}{T_0},\ c_0=\sqrt{\frac{E}{\rho}}.\\ \{t',\tau'_\theta\}=\frac{c_0}{\mathrm{L}}\{t,\tau_\theta\},\ \sigma'_x=\frac{\sigma_x}{E},\ M'=\frac{M}{ALE}.\end{gathered} \tag{15}$$

Then, the fundamental equations are reduced to nondimensional forms as

$$\begin{gathered}\frac{\partial^4 w}{\partial x^4}-B_1\frac{\partial^2 w}{\partial x^2}+B_2\frac{\partial^2 w}{\partial t^2}+B_3 w=-B_4\frac{\partial^2\theta}{\partial x^2}\\ \left(K\frac{\partial}{\partial t}+K^*\right)\left(\frac{\partial^2}{\partial x^2}-B_5\right)\theta=\left(\frac{\partial^2}{\partial t^2}+\tau_\theta\frac{\partial^3}{\partial t^3}\right)\left[B_6\frac{\partial\theta}{\partial t}-B_7\frac{\partial}{\partial t}\left(\frac{\partial^2 w}{\partial x^2}\right)\right],\end{gathered} \tag{16}$$

$$M(x,t)=-A_8\frac{\partial^2 w(x,t)}{\partial x^2}-A_9\theta. \tag{17}$$

Anywhere

$$\begin{bmatrix} A_1 \\ A_2 \\ A_3 \end{bmatrix} = \begin{bmatrix} L^2\left(\frac{12K_2}{h^3bE} + \frac{12\mu_0 H_x^2}{h^2E}\right) \\ \frac{12L^2}{h^2} \\ \frac{12L^4K_1}{bh^3E} \end{bmatrix}, \begin{bmatrix} A_4 \\ A_5 \\ A_6 \end{bmatrix} = \begin{bmatrix} \frac{24\mathrm{L}T_0\alpha_T}{h\pi^2} \\ \frac{L^2\pi^2}{h^2} \\ \frac{L}{k}\sqrt{\frac{E}{\rho}} \end{bmatrix} \text{ and } \begin{bmatrix} A_7 \\ A_8 \\ A_9 \end{bmatrix} = \begin{bmatrix} \frac{\gamma\pi^2 h}{24K}\sqrt{\frac{E}{\rho}} \\ \frac{h^2}{12bL^2} \\ \frac{2\mathrm{h}T_0\alpha_T}{L\pi^2} \end{bmatrix}.$$

Now, we investigate the initial and boundary conditions necessary to clarify the issue. The original uniform conditions are expressed as

$$\theta(x,0) = \frac{\partial \mathrm{T}(x,0)}{\partial t} = 0 = w(x,0) = \frac{\partial w(x,0)}{\partial t}. \tag{18}$$

We deliberate that the microbeam is clamped at both ends, i.e.,

$$w(0,t) = w(L,t) = 0 = \frac{\partial^2 w(0,t)}{\partial x^2} = \frac{\partial^2 w(L,t)}{\partial x^2}. \tag{19}$$

Furthermore, we consider that slope-type heating thermally loads the microbeam, which provides

$$\theta(x,t) = \mathrm{T}_0 \begin{cases} 0, & t \le 0 \\ \frac{t}{t_0}, & 0 \le t \le t_0, \\ 1, & t > 0 \end{cases} \tag{20}$$

where T_0 is a constant and t_0 is a slope-type parameter. Moreover, the following connection must be satisfied by the temperature at the end boundary [29,30]:

$$\frac{\partial \theta}{\partial x} = 0 \text{ on } x = L. \tag{21}$$

4. Solution of the problem in the Laplace transform domain

The Laplace transform is defined as

$$\bar{g}(x,t) = \int_0^\infty g(x,t)e^{-st}dt. \tag{22}$$

Under homogeneous initial conditions (18) and on both sides of Eqs (16) and (17), we can obtain the field equations in the Laplace transform space as follows:

$$\begin{gathered} \frac{\mathrm{d}^4\bar{w}}{\mathrm{d}x^4} - A_{10}\frac{\mathrm{d}^2\bar{w}}{\mathrm{d}x^2} + A_{11}\bar{w} = -A_{12}\frac{\mathrm{d}^2\bar{\theta}}{\mathrm{d}x^2} \\ \left(\frac{\mathrm{d}^2}{\mathrm{d}x^2} - A_{13}\right)\bar{\theta} = -A_{14}\frac{\mathrm{d}^2\bar{w}}{\mathrm{d}x^2}, \end{gathered} \tag{23}$$

$$\bar{M}(x,s) = -A_{15}\frac{\mathrm{d}^2\bar{w}}{\mathrm{d}x^2} - A_{16}\bar{\theta}, \tag{24}$$

wherever

$$\begin{bmatrix} A_{10} \\ A_{11} \\ A_{12} \end{bmatrix} = \begin{bmatrix} A_1 \\ s^2 A_2 + A_3 \\ A_4 \end{bmatrix} \text{ and } \begin{bmatrix} A_{13} \\ A_{14} \\ A_{15} \\ A_{16} \end{bmatrix} = \begin{bmatrix} A_5 + A_6 \frac{(s^2+\tau_\theta s^3)}{(Ks+K^*)} \\ A_7 \frac{(s^2+\tau_\theta s^3)}{(Ks+K^*)} \\ A_8 \\ A_9 \end{bmatrix}.$$

When $\bar{\theta}$ or $\bar{w}$ is eliminated from Eq (23), one becomes:

$$(D^6 - C_1 D^4 + C_2 D^2 - C_3)\{\bar{w}, \bar{\theta}\}(x) = 0, \tag{25}$$

where C_1, C_2, and C_3 are given in (26)

$$\begin{bmatrix} C_1 \\ C_2 \\ C_3 \\ D \end{bmatrix} = \begin{bmatrix} A_{10} + A_{14} + A_{12}A_{14} \\ A_{10}A_{14} + A_{11} \\ A_{11}A_{14} \\ \frac{d}{dx} \end{bmatrix}. \tag{26}$$

Equation (27) can be improved to

$$(D^2 - m_1^2)(D^2 - m_2^2)(D^2 - m_3^2)\{\bar{w}, \bar{\theta}\}(x) = 0. \tag{27}$$

where μ_i^2 and $i = 1,2,3,4$ are the roots of

$$\mu^6 - C_1\mu^4 + C_2\mu^2 - C_3 = 0. \tag{28}$$

In the domain of the Laplace transform, the solution to Eq (28) can be described as

$$\{\bar{w}, \bar{\theta}\}(x) = \sum_{i=1}^{3}(\{1, \lambda_i\}A_i e^{-\mu_i x} + \{1, \lambda_{i+3}\}A_{i+3} e^{\mu_i x}). \tag{29}$$

When these two equations agree with Eq (24), we obtain

$$\lambda_i = -\frac{\mu_i^2 A_{14}}{\mu_i^2 - A_{13}}. \tag{30}$$

Equation (29) is used to obtain the displacement regarding

$$\bar{u}(x) = -z\frac{d\bar{w}}{dx} = z\sum_{i=1}^{3}\mu_i(A_i e^{-\mu_i x} - A_{i+3} e^{\mu_i x}). \tag{31}$$

The value for moment $\bar{M}$ can be created by substituting the equations of $\bar{w}$ and $\bar{\theta}$ from Eq (29) into Eq (25):

$$\bar{M}(x) = -\sum_{i=1}^{3}(\mu_i^2 A_{15} + A_{16}\lambda_i)(A_i e^{-\mu_i x} - A_{i+3} e^{\mu_i x}). \tag{32}$$

Additionally, the strain will be

$$\bar{e}(x) = \frac{d\bar{u}}{dx} = -z\sum_{i=1}^{3}\mu_i^2(A_i e^{-\mu_i x} - A_{i+3} e^{\mu_i x}). \tag{33}$$

When the Laplace transform is used, boundary conditions (18)–(20) take the following forms:

$$\begin{gathered}\overline{w}(0,s)=\overline{w}(L,s)=0,\\ \frac{\partial^2\overline{w}(0,s)}{\partial x^2}=\frac{\partial^2\overline{w}(L,s)}{\partial x^2}=0,\\ \frac{\partial\overline{\theta}(0,s)}{\partial x}=\mathrm{T}_0\left(\frac{1-e^{-s\tau_\theta}}{s^2\,\tau_\theta}\right),\\ \frac{\partial\overline{\theta}(L,s)}{\partial x}=0.\end{gathered} \tag{34}$$

By replacing the previous boundary conditions with Eq (29), six linear equations are formed.

$$\begin{gathered}\sum_{i=1}^{3}(A_i+A_{i+1})=0,\\ \sum_{i=1}^{3}(A_ie^{-\mu_iL}+A_{i+1}e^{\mu_iL})=0.\end{gathered} \tag{35}$$

$$\begin{gathered}\sum_{i=1}^{3}\mu_i^2(A_i+A_{i+1})=0,\\ \sum_{i=1}^{3}\mu_i^2(A_ie^{-\mu_iL}+A_{i+1}e^{\mu_iL})=0.\end{gathered} \tag{36}$$

$$\begin{gathered}\sum_{i=1}^{3}\mu_i(\lambda_iA_i-\lambda_{i+1}A_{i+1})=-\mathrm{T}_0\left(\frac{1-e^{-s\tau_\theta}}{s^2\,\tau_\theta}\right).\\ \sum_{i=1}^{3}\mu_i(\lambda_iA_ie^{-\mu_iL}-\lambda_{i+1}A_{i+1}e^{\mu_iL})=0.\end{gathered} \tag{37}$$

The aforementioned system of linear equations $(i=1,2,\ldots,6)$ is solved to obtain the unknown parameters A_i. The Riemann sum approximation method is used to obtain numerical results for physical domain research areas.

5. Numerical results

This section compares the findings of the MGT with the KG model to those of the CTE, LS, GN-II, and GN-III models. Additionally, via the theoretical analysis described in the preceding sections, the impacts of the distributions of temperature, displacement, deflection, and flexure moments on the scale parameter $\boldsymbol{e_0}$ are evaluated. Our findings contrast with those of earlier studies in Figures 1–8. The geometrical and physical properties of the microbeam are shown below in [45].

$$K(\mathrm{Wm^{-1}K^{-1}})=156,\qquad \nu=0.22,\qquad T_0=293\mathrm{K},$$

$$E(GP\mathrm{a})=169,\qquad \rho(\mathrm{Kgm^{-3}})=2330,\qquad \alpha_{\mathrm{t}}(\mathrm{K^{-1}})=2.59\times10^{-6},$$

$$k(\mathrm{m^2s^{-1}})=9.4\times10^{-5},\qquad C_E\left(\frac{\mathrm{J}}{\mathrm{kgK}}\right)=713.$$

5.1. The effects of different models of thermoelasticity

Numerous observations are presented in this part to computationally compare several thermoelastic models. This is accomplished by varying the displacement, temperature, deflection, and flexure moment with respect to distance r for the models CTE, LS, GN-II, GN-III, MGT, and KG. Figures 1–4 show our findings.

In Figure 1, temperature variations θ are explained by the Moore–Gibson–Thomson thermoelastic model MGT with KG nonlocality, the Green–Naghde models (GN-II and GN-III), the Lord–Shulman thermodynamic model (LS), and the classical thermodynamic model (CTE). First,

there is variation in magnitude across these models. All the models have greater starting temperatures that progressively decrease over time. Additionally, during the micropacket period, the CTE, LS, GN-II, GN-III, MGT, and KG models show comparable distributions before converging to zero. These findings align with those of the research conducted by [40].

In Figure 2, the displacement u against the distance r is plotted to compare the different models. In the LS model, the displacement u is equal to that of the GN-III, MGT, and KG models, whereas the displacement u in the CTE and GN-II models differs from those in the GN-III, MGT, and KG models. Compared with those of the other generalized models, the displacement curves in the interval $(0 \leq r \leq 0.2)$ exhibit lower values for the CTE and GN-II models. Furthermore, we observe that the six models CTE, LS, GN-II, GN-III, MGT, and KG provide negative values in the interval $(0.2 \leq r \leq 1.4)$ and converge to zero. The thermoelastic model and material parameters are crucial for predicting the anticipated displacement. The most sensitive material was the one that exhibited the greatest change in response to a stimulus during the experiment. The model that best aligns with the experimental data is preferable for predicting material behavior.

Figure 3 illustrates the distribution of thermoelastic vibration with deflection W for the different models (CTE, LS, GN-II, GN-III, MGT, and KG). We see that the distribution of thermoelastic with deflection W for GN-III, MGT, and KG is larger than that of CTE, LS, and GN-II. All the models reach the lowest values in the interval $(0 \leq r \leq 0.4)$. Similarly, the five models CTE, LS, GN-II, GN-III, and MGT slowly fade inside the microbeams until they settle at zero in the interval $(1.4 \leq r \leq 2)$. Additionally, Figure 3 elucidates the predictions of variations in deviation (w) via various thermoelastic models for the same material. The material exhibiting the most incredible sensitivity may be discerned by juxtaposing these models with experimental outcomes for several materials.

Figure 4 illustrates the distribution of thermoelastic vibration with the moment M for the different models (CTE, LS, GN-II, GN-III, MGT, and KG). The moment M curves in period $(0 \leq r \leq 2)$ have lower values in the CTE and GN-III models than in the other generalized models, but have larger values in the MGT and KG models. The discrepancies in the predicted bending moments serve as indicators of how each model understands the interaction between mechanical and thermal reactions. While some models provide more stable predictions, others show substantial changes in the bending moment due to their assumptions regarding thermal coupling and propagation.

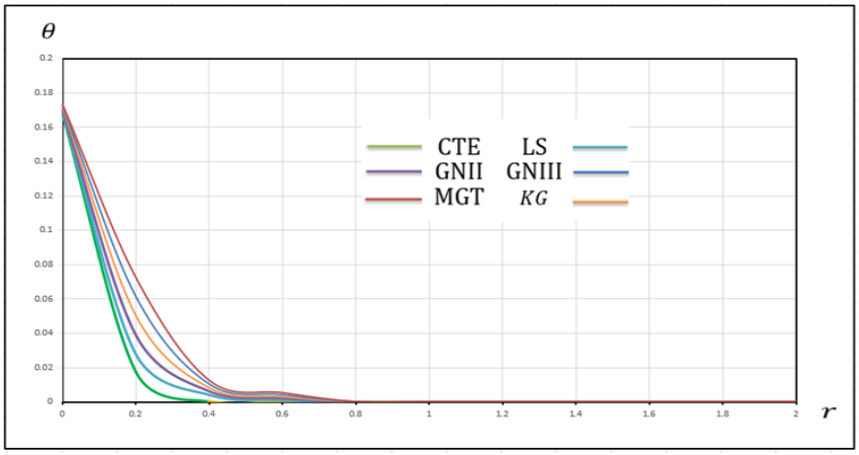

Figure 1. Temperature θ in different models of thermoelasticity.

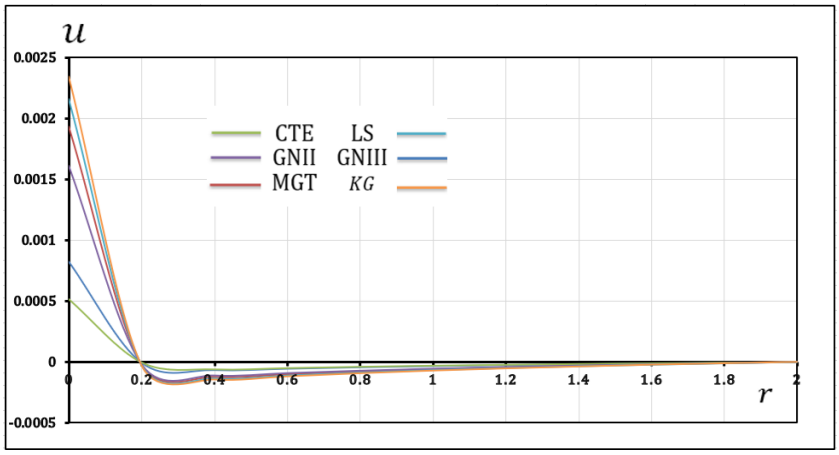

Figure 2. Displacement u in different models of thermoelasticity.

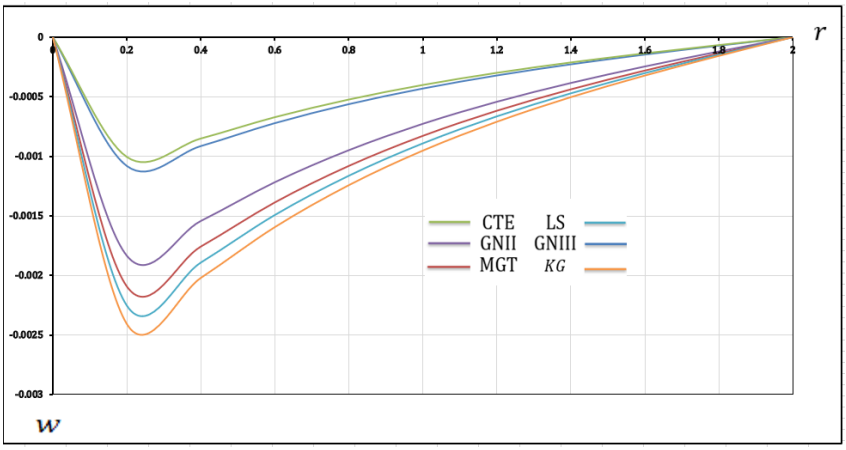

Figure 3. Deflection w in different models of thermoelasticity.

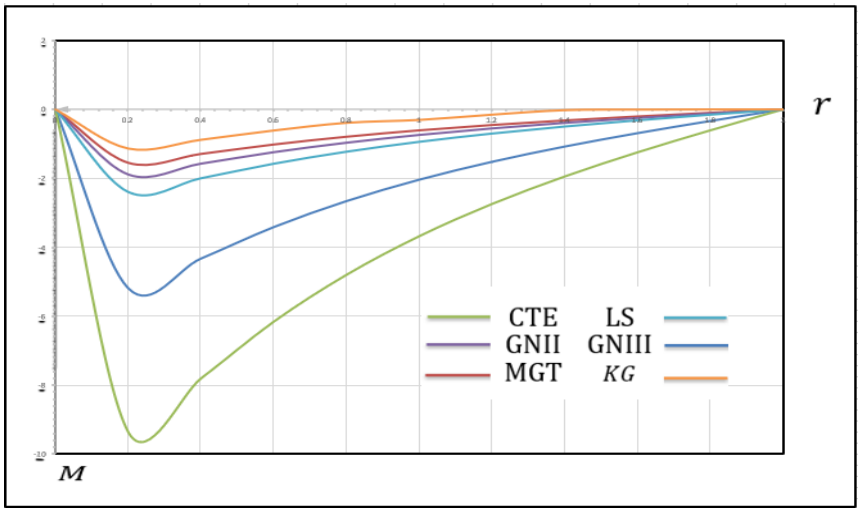

Figure 4. Moment M in different models of thermoelasticity.

5.2. Effect of Pasternak foundation parameters K_1 *and* K_2

This section focuses on the analytical and numerical analysis of the influence of the Pasternak foundation parameters K_1 and K_2 on the beam response. The effects of the Pasternak foundation parameters on the behavior of the microbeam are shown in Figures 5–8.

Since the Pasternak foundation model better captures the continuous character of the foundation, it is often applied in practice. Figures 5–8 demonstrate how different parameters K_1 and K_2 impact field values such as Θ, u, w, and M. A comparative analysis was performed to validate the present study. The statistics reveal that the four locations are in sync. The microbeam becomes stiffer when supported by an elastic foundation. The basic parameters K_1 and K_2 strongly impact the bending moment M, displacement u, and deflection w. We may also conclude the following: As in [7,8,40], both parameters reduced deflection, increased thermal coupling, and improved microbeam structural integrity; structures supported by a mix of Winkler and Pasternak foundations are stiffer than those supported by only one.

These cases in Figure 5 exhibit varying magnitudes, and it is evident that the starting temperature values are larger and progressively decrease over time in every case, with lower temperatures in $K_1 = 0.1,\ K_2 = 0$. Moreover, before convergence to zero, the cases where $K_1 = 0,\ K_2 = 0.05,\ K_1 = 0.1,\ K_2 = 0$ and $K_1 = 0.1,\ K_2 = 0.05$ have equivalent distributions, indicating a strong effect of temperature θ-dependent characteristics on the distributions of physical quantities.

The displacement u achieves its largest value in the cases where $K_1 = 0,\ K_2 = 0.05,\ K_1 = 0.1, K_2 = 0$ and $K_1 = 0.1,\ K_2 = 0.05$, as shown in Figure 6, which is different from the case where $K_1 = 0.1,\ K_2 = 0$. The two cases $K_1 = 0,\ K_2 = 0.05,\ K_1 = 0.1,\ K_2 = 0$ and $K_1 = 0.1,\ K_2 = 0.05$ also show comparable curves and near values; however, case $K_1 = 0.1,\ K_2 = 0$ is completely different. All three cases' curves progressively fade until they settle at zero in $(1.2 < x < 2)$.

The deflection w achieves its maximum value in the case of $K_1 = 0.1, K_2 = 0$, as shown in Figure 7, diverging from $K_1 = 0,\ K_2 = 0.05,\ K_1 = 0.1, K_2 = 0$ and $K_1 = 0.1,\ K_2 = 0.05$.

Figure 8 shows the distribution of the moment M for several cases. The curve is lower in the $K_1 = 0.1,\ K_2 = 0$ case than in the $K_1 = 0,\ K_2 = 0.05,\ K_1 = 0.1, K_2 = 0$ and $K_1 = 0.1,\ K_2 = 0.05$ cases.

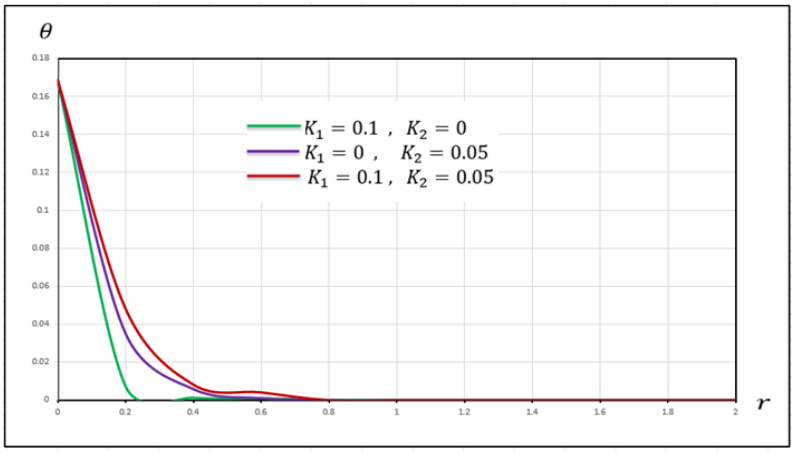

Figure 5. Temperature θ with different Pasternak foundation parameters K_1 and K_2.

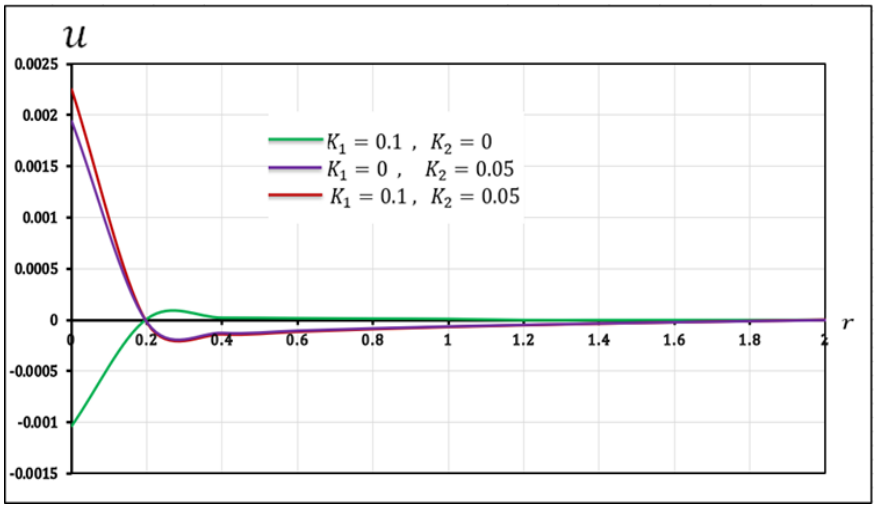

Figure 6. Displacement u with different Pasternak foundation parameters $\boldsymbol{K_1}$ and $\boldsymbol{K_2}$.

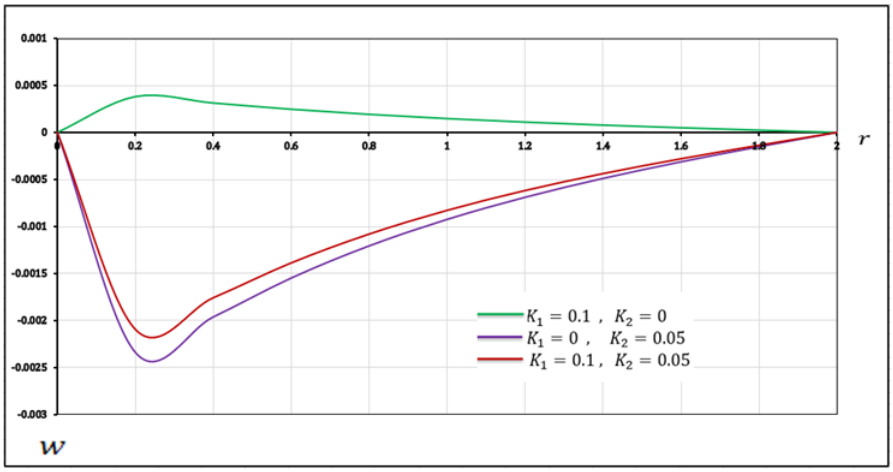

Figure 7. Deflection w with different Pasternak foundation parameters $\boldsymbol{K_1}$ and $\boldsymbol{K_2}$.

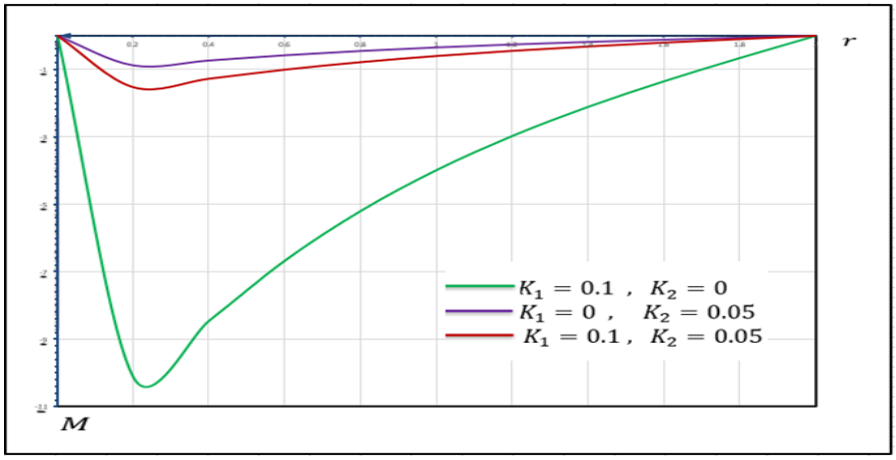

Figure 8. Moment M with different Pasternak foundation parameters $\boldsymbol{K_1}$ and $\boldsymbol{K_2}$.

5.3. Effect scale parameter $\boldsymbol{e_0}$

In particular, the dynamics of microbeams processed via a two-parameter viscoelastic Pasternak foundation may be more accurately represented by including the Klein–Gordon operator in the theoretical analysis. This technique successfully addresses size-dependent phenomena that are usually disregarded by traditional local elasticity theories by considering the nonlocal length scale e_0 and time scale τ factors. Because of the considerable influence of spatial and temporal interactions on the mechanical and thermal characteristics of thermoelastic materials, these advancements are crucial for comprehending these materials.

By including nonlocal length scale (e_0) and time scale (τ) variables, the importance of nonlocal characteristics in thermoelastic material modeling is highlighted. Spatial nonlocality, as shown by the length scale e_0, means that stress or strain in one location is affected by stress or strain in neighboring places. For the model to anticipate dimensionally dependent behaviors, such as lower stiffness or wave dispersion, this feature is crucial for including size effects. Particularly important for microbeams treated with a two-parameter viscoelastic Pasternak foundation is the influence of e_0, which takes into account the effects of long-range forces and atomic-scale interactions. In addition, the model incorporates vibration effects via the parameter τ, which represents temporal nonlocality. This is crucial for recording how a material might *cohere* with its past states, which affects how it responds now.

The total amount of strain and stress decreases because the spatial nonlocality parameter e_0 takes into account the influence of neighboring stresses and strains. These size-dependent behaviors are introduced by this smoothing effect, which also reduces variability. These adjustments allow for a more precise depiction of the physical behavior of a microbeam, where interactions with respect to the atomic size are very important. The capacity of the material to gradually adjust to changes over time is reflected by the temporal nonlocality parameter τ, which allows the model to account for damping effects and postpone wave propagation. Given the critical role that relaxation effects play in determining the reactions of viscoelastic and thermoelastic materials, this aspect demands particular attention. The results obtained by [40,45] agree with this finding. This section aims to determine how the scale parameter $\boldsymbol{\tau_\theta}$ affects the examined field measures. For comparison with other studies, findings are shown in Figures 9–12. The distribution of the physical fields has a noticeable influence on the scale parameter e_0.

We conclude that increasing parameters K_1 and K_2 increases the temperature θ values on the basis of the data presented in Figure 9. Additionally, the value of e_0 has important effects on temperature over a wide range of r, i.e., $(0 < r < 0.2)$; increasing the value of e_0 causes a decrease in the value of temperature θ. Until crossing the r-axis, the displacement begins with positive values, progressively decreases, and then takes positive values until essentially approaching zero. Figure 10 shows a graph that shows the effect of the scale parameter e_0 on the sensitivity of the displacement u of microbeams processed via a two-parameter viscoelastic Pasternak foundation and a Moore–Gibson–Thompson heat conduction model with KG nonlocality. All of the values of displacement u are convergent, according to the data displayed in this figure. Figure 11 shows that the deflection w starts decreasing with the scale parameter e_0 in the range $0 \le r \le 0.3$ and then increases to maximum amplitudes in the range $0.3 \le r \le 2$. Figure 12 shows how the moment M presents several curves depending on the scale parameter e_0, which ranges from $0 \le r \le 2$.

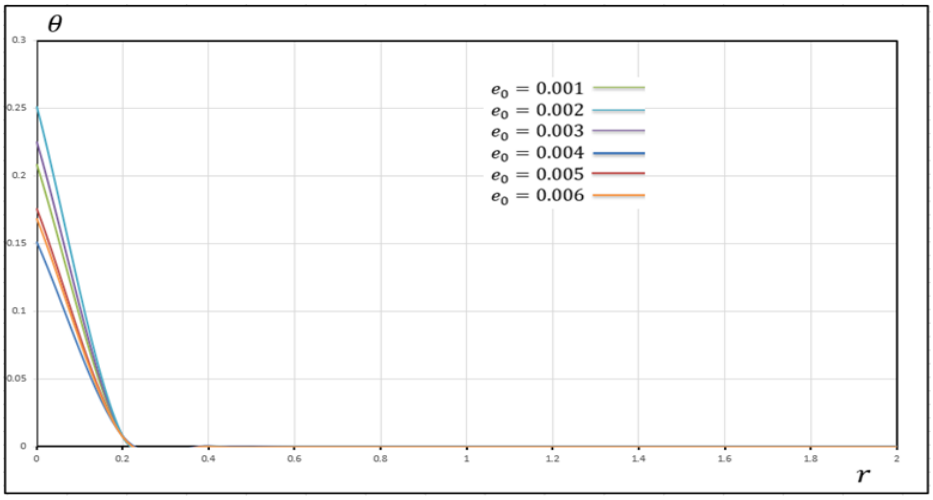

Figure 9. Temperature θ with different scale parameters e_0.

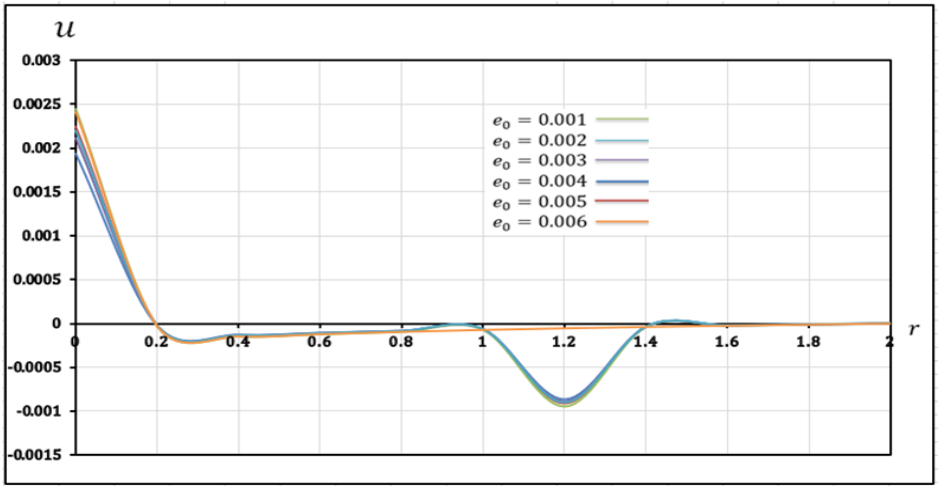

Figure 10. Displacement u with different scale parameters e_0.

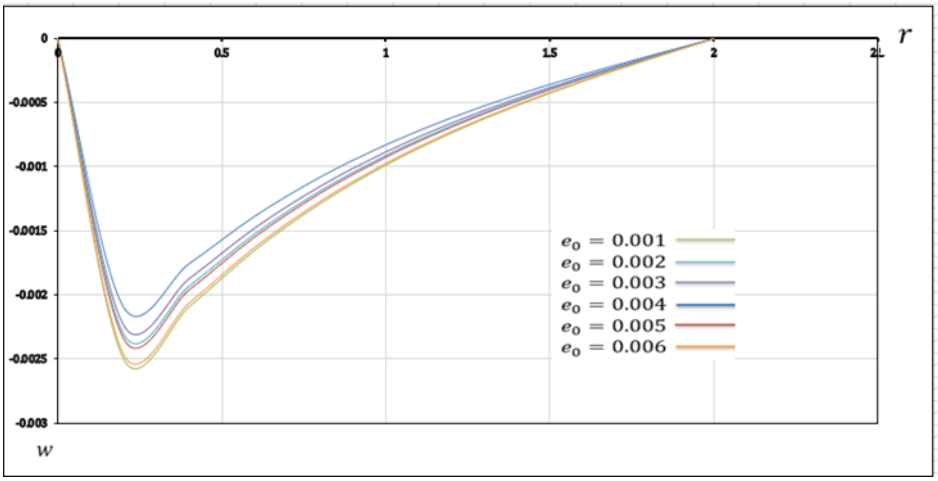

Figure 11. Deflection w with different scale parameters e_0.

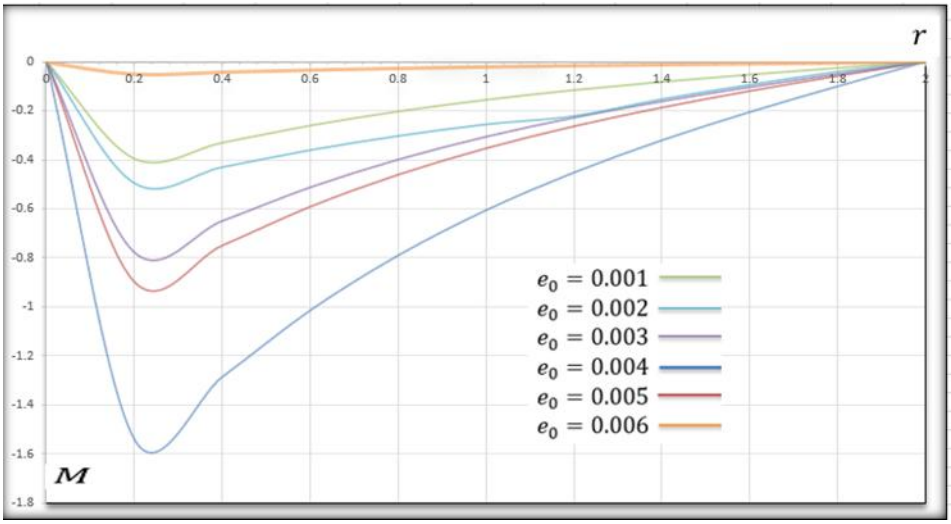

Figure 12. Moment M with different scale parameters e_0.

6. Conclusions

This work uses the Moore–Gibson–Thompson model with KG nonlocality to analyze the displacement, temperature, deflection, and flexure moment of thermoelastic microbeam resonators under the influence of a two-parameter viscoelastic Pasternak foundation. The normalized versions of the governing equations were compared with those of thermoelastic models (CTE, LS, GN-II, GN-III, MGT, and KG) and different scale characteristics of microbeams in terms of displacement, temperature, deflection, and flexure moment. The important findings from this study include the following:

- These models primarily display variations in their magnitudes, and the initial temperature values are relatively high, gradually decreasing over time intervals across all the models.
- The amplitudes of displacement and deflection under all six models, namely, CTE, LS, GN-II, GN-III, MGT, and KG, are approximately the same.
- Greater values are obtained under the GN-III, MGT, and KG models, but lower values are obtained for the moment in the GN-II, LS, and CTE models.
- In the cases where $K_1 = 0,\ K_2 = 0.05$ and $K_1 = 0.1,\ K_2 = 0.05$, higher values are obtained for temperature, displacement, and moment, but in the cases where $(K_1 = 0.1, K_2 = 0)$, higher values are found for deflection.
- The moment displays several curves depending on the scale parameter, and the temperature increases as two parameters, K_1 and K_2, increase. The deflection and displacement values tend to decrease when two parameters, K_1 and K_2, encounter more difficulties.
- The nonlocal Klein–Gordon parameter effects are prominent in high-frequency and short-wavelength waves to capture factors that classical elasticity cannot account for.
- The Moore–Gibson–Thompson model, under the effect of the nonlocal KG model, has been applied to general thermoelastic problems by many researchers in the field of generalized thermoelasticity. However, to the best of the authors' knowledge, it has not been applied to thermoelastic microbeams supported by a two-parameter Pasternak basis.

Author contributions

Ahmed Yahya: Drafting and designing the article; formal analysis; data interpretation; critical revision; final approval of the published version. Adam Zakria and Shams A. Ahmed: original draft writing, study design, methodology, article revision through critical analysis, and final approval of the published version. Husam E. Dargail and Ibrahim-Elkhalil Ahmed: Study design; methodology; data collection and acquisition; writing; initial draft; critical revision; final approval of the published version. Abdelgabar Adam Hassan and Eshraga Salih: Data collection and acquisition, formal analysis, data interpretation, original draft writing, and final approval of the version that will be published. All the authors have read and approved the final version of the manuscript for publication.

Use of Generative-AI tools declaration

The authors declare they have not used Artificial Intelligence (AI) tools in the creation of this article.

Conflict of interest

The authors declare that none of the work reported in this paper could have been influenced by any known competing financial interests or personal relationships.

References

1. X. Zhao, W. D. Zhu, Y. H. Li, Analytical solutions of nonlocal coupled thermoelastic forced vibrations of micro-/nano-beams by means of Green's functions, *J. Sound Vib.*, **481** (2020), 115407. https://doi.org/10.1016/j.jsv.2020.115407
2. Z. Adam, A. Yahya, A. E. Abouelregal, M. Suhail, Vibration analysis of thermoelastic microbeams on a Pasternak foundation with two parameters using the Moore–Gibson–Thompson heat conduction model, *Continuum Mech. Thermodyn.*, **37** (2025), 27. https://doi.org/10.1007/s00161-025-01358-z
3. Y. Sun, D. Fang, A. K. Soh, Thermoelastic damping in micro-beam resonators, *Int. J. Solids Struct.*, **43** (2006), 3213–3229. https://doi.org/10.1016/j.ijsolstr.2005.08.011
4. K. Ramachandran, V. Boopalan, J. C. Bear, R. Subramani, Multi-walled carbon nanotubes (MWCNTs)-reinforced ceramic nanocomposites for aerospace applications: a review, *J. Mater. Sci.*, **57** (2022), 3923–3953. https://doi.org/10.1007/s10853-021-06760-x
5. P. Zahedinejad, C. Zhang, H. Zhang, S. Ju, A comprehensive review on vibration analysis of functionally graded beams, *Int. J. Struct. Stab. Dyn.*, **20** (2020), 2030002. https://doi.org/10.1142/S0219455420300025
6. M. Kandaz, H. Dal, A comparative study of modified strain gradient theory and modified couple stress theory for gold microbeams, *Arch. Appl. Mech.*, **88** (2018), 2051–2070. https://doi.org/10.1007/s00419-018-1436-0
7. B. Zhao, T. Liu, J. Chen, X. Peng, Z. Song, A new Bernoulli–Euler beam model based on modified gradient elasticity, *Arch. Appl. Mech.*, **89** (2019), 277–289. https://doi.org/10.1007/s00419-018-1464-9

8. X. Liang, S. Hu, S. Shen, A new Bernoulli–Euler beam model based on a simplified strain gradient elasticity theory and its applications, *Compos. Struct.*, **111** (2014), 317–323. https://doi.org/10.1016/j.compstruct.2014.01.019
9. O. Doeva, P. K. Masjedi, P. M. Weaver, Closed form solutions for an anisotropic composite beam on a two-parameter elastic foundation, *Eur. J. Mech.-A/Solids*, **88** (2021), 104245. https://doi.org/10.1016/j.euromechsol.2021.104245
10. U. Bhattiprolu, A. K. Bajaj, P. Davies, An efficient solution methodology to study the response of a beam on viscoelastic and nonlinear unilateral foundation: static response, *Int. J. Solids Struct.*, **50** (2013), 2328–2339. https://doi.org/10.1016/j.ijsolstr.2013.03.014
11. A. E. Abouelregal, I. Dassios, O. Moaaz, Moore–Gibson–Thompson thermoelastic model effect of laser-induced microstructures of a microbeam sitting on Visco-Pasternak foundations, *Appl. Sci.*, **12** (2022), 9206. https://doi.org/10.3390/app12189206
12. S. Pradhan, T. Murmu, Thermo-mechanical vibration of FGM sandwich beam under variable elastic foundations using differential quadrature method, *J. Sound Vib.*, **321** (2009), 342–362. https://doi.org/10.1016/j.jsv.2008.09.018
13. M. A. Biot, Thermoelasticity and irreversible thermodynamics, *J. Appl. Phys.*, **27** (1956), 240–253. https://doi.org/10.1063/1.1722351
14. H. W. Lord, Y. Shulman, A generalized dynamical theory of thermoelasticity, *J. Mech. Phys. Solids*, **15** (1967), 299–309. https://doi.org/10.1016/0022-5096(67)90024-5
15. A. E. Green, K. Lindsay, Thermoelasticity, *J. Elast.*, **2** (1972), 1–7. https://doi.org/10.1007/BF00045689
16. A. Green, P. Naghdi, Thermoelasticity without energy dissipation, *J. Elast.*, **31** (1993), 189–208. https://doi.org/10.1007/BF00044969
17. M. A. Biot, D. G. Willis, The elastic coefficients of the theory of consolidation, *J. Appl. Mech.*, **24** (1957), 594–601. https://doi.org/10.1115/1.4011606
18. D. Y. Tzou, The generalized lagging response in small-scale and high-rate heating, *Int. J. Heat Mass Tran.*, **38** (1995), 3231–3240. https://doi.org/10.1016/0017-9310(95)00052-B
19. A. E. Green, P. Naghdi, A re-examination of the basic postulates of thermomechanics, *Proc. R. Soc. Lond. Ser. A*, **432** (1991), 171–194. https://doi.org/10.1098/rspa.1991.0012
20. A. E. Green, P. M. Naghdi, On undamped heat waves in an elastic solid, *J. Thermal Stresses*, **15** (1992), 253–264. https://doi.org/10.1080/01495739208946136
21. B. Kaltenbacher, I. Lasiecka, R. Marchand, Wellposedness and exponential decay rates for the Moore-Gibson-Thompson equation arising in high intensity ultrasound, *Control Cybern.*, **40** (2011), 971–988.
22. F. Dell'Oro, I. Lasiecka, V. Pata, The Moore–Gibson–Thompson equation with memory in the critical case, *J. Differ. Equations*, **261** (2016), 4188–4222. https://doi.org/10.1016/j.jde.2016.06.025
23. I. Lasiecka, X. Wang, Moore–Gibson–Thompson equation with memory, part II: general decay of energy, *J. Differ. Equations*, **259** (2015), 7610–7635. https://doi.org/10.1016/j.jde.2015.08.052
24. M. Conti, V. Pata, R. Quintanilla, Thermoelasticity of Moore–Gibson–Thompson type with history dependence in the temperature, *Asymptotic Anal.*, **120** (2020), 1–21. https://doi.org/10.3233/ASY-191576
25. R. Quintanilla, Moore–Gibson–Thompson thermoelasticity, *Math. Mech. Solids*, **24** (2019), 4020–4031. https://doi.org/10.1177/1081286519862007

26. N. Bazarra, J. R. Fernández, R. Quintanilla, Analysis of a Moore–Gibson–Thompson thermoelastic problem, *J. Comput. Appl. Math.*, **382** (2021), 113058. https://doi.org/10.1016/j.cam.2020.113058
27. D. G. B. Edelen, N. Laws, On the thermodynamics of systems with nonlocality, *Arch. Rational Mech. Anal.*, **43** (1971), 24–35. https://doi.org/10.1007/BF00251543
28. D. G. B. Edelen, A. E. Green, N. Laws, Nonlocal continuum mechanics, *Arch. Rational Mech. Anal.*, **43** (1971), 36–44. https://doi.org/10.1007/BF00251544
29. H. Zhou, X. Song, P. Li, Generalized thermoelastic dissipation in micro/nano-beams with two-dimensional heat conduction, *Int. J. Mech. Sci.*, **252** (2023), 108371. https://doi.org/10.1016/j.ijmecsci.2023.108371
30. X. Song, P. Li, H. Zhou, Generalized frequency shift and attenuation in simply-supported micro/nano-beam resonators with thermoelastic dissipation, *J. Therm. Stresses*, **47** (2024), 395–417. https://doi.org/10.1080/01495739.2023.2301609
31. A. C. Eringen, Linear theory of nonlocal elasticity and dispersion of plane waves, *Int. J. Eng. Sci.*, **10** (1972), 425–435. https://doi.org/10.1016/0020-7225(72)90050-X
32. D. Singh, G. Kaur, S. K. Tomar, Waves in nonlocal elastic solid with voids, *J. Elast.*, **128** (2017), 85–114. https://doi.org/10.1007/s10659-016-9618-x
33. A. C. Eringen, Theory of nonlocal thermoelasticity, *Int. J. Eng. Sci.*, **12** (1974), 1063–1077. https://doi.org/10.1016/0020-7225(74)90033-0
34. F. Balta, E. S. Şuhubi, Theory of nonlocal generalized thermoelasticity, *Int. J. Eng. Sci.*, **15** (1977), 579–588. https://doi.org/10.1016/0020-7225(77)90054-4
35. S. Biswas, Rayleigh waves in a nonlocal thermoelastic layer lying over a nonlocal thermoelastic half-space, *Acta Mech.*, **231** (2020), 4129–4144. https://doi.org/10.1007/s00707-020-02751-2
36. P. Lata, S. Singh, Rayleigh wave propagation in a nonlocal isotropic magneto-thermoelastic solid with multi-dual-phase lag heat transfer, *Int. J. Geomath.*, **13** (2022), 5. https://doi.org/10.1007/s13137-022-00195-5
37. A. M. Abd-Alla, S. M. Abo-Dahab, S. M. Ahmed, M. M. Rashid, Effect of magnetic field and voids on Rayleigh waves in a nonlocal thermoelastic half-space, *J. Strain Anal. Eng. Des.*, **57** (2021), 61–72. https://doi.org/10.1177/03093247211001243
38. K. Jangid, M. Gupta, S. Mukhopadhyay, On propagation of harmonic plane waves under the Moore–Gibson–Thompson thermoelasticity theory, *Waves Random Complex Media*, **34** (2021), 1976–1999. https://doi.org/10.1080/17455030.2021.1949071
39. R. Quintanilla, Moore–Gibson–Thompson thermoelasticity with two temperatures, *Appl. Eng. Sci.*, **1** (2020), 100006. https://doi.org/10.1016/j.apples.2020.100006
40. M. Lazer, E Agiasofal, Nonlocal elasticity of Klein–Gordon type: fundamentals and wave propagation, *Wave Motion*, **114** (2022), 103038. https://doi.org/10.1016/j.wavemoti.2022.103038
41. O. A. Bauchau, J. I. Craig, Euler–Bernoulli beam theory, In: O. A. Bauchau, J. I. Craig, *Structural analysis*, Solid Mechanics and Its Applications, Springer, **163** (2009), 173–221. https://doi.org/10.1007/978-90-481-2516-6_5
42. O. Aldraihem, R. Wetherhold, T. Singh, Intelligent beam structures: Timoshenko theory vs. Euler-Bernoulli theory, *Proceeding of the 1996 IEEE International Conference on Control Applications IEEE International Conference on Control Applications held together with IEEE International Symposium on Intelligent Contro*, 1996, 976–981. https://doi.org/10.1109/CCA.1996.559047
43. X. Wang, R. Therefore, Y. Liu, Flow-induced vibration of an Euler–Bernoulli beam, *J. Sound Vib.*, **243** (2001), 241–268. https://doi.org/10.1006/jsvi.2000.3342

44. A. D. Kerr, A study of a new foundation model, *Acta Mech.*, **1** (1965), 135–147. https://doi.org/10.1007/BF01174308
45. A. Zakria, O. A. A. Osman, M. Suhail, M. N. A. Rabih, Fractional Moore–Gibson–Thompson heat conduction for vibration analysis of non-local thermoelastic Micro-Beams on a viscoelastic Pasternak foundation, *Fractal Fract.*, **9** (2025), 118. https://doi.org/10.3390/fractalfract9020118

AIMS Press